P-Glycoprotein Antibody Functionalized Carbon Nanotube Overcomes the Multidrug Resistance of Human Leukemia Cells

Ruibin Li,[†] Ren'an Wu,[†,*] Liang Zhao,[†] Minghuo Wu,[†] Ling Yang,[‡] and Hanfa Zou[†,*]

[†]National Chromatographic R&A Center, CAS Key Laboratory of Separation Sciences for Analytical Chemistry and [‡]Laboratory of Pharmaceutical Resource Discovery, Dalian Institute of Chemical Physics, Chinese Academy of Sciences (CAS), Dalian 116023, China

ABSTRACT Multidrug resistance (MDR), which is related to cancer chemotherapy, tumor stem cells, and tumor metastasis, is a huge obstacle for the effective cancer therapy. One of the underlying mechanisms of MDR is the increased efflux of anticancer drugs by overexpressed P-glycoprotein (P-gp) of multidrug resistant cells. In this work, the antibody of P-gp (anti-P-gp) functionalized water-soluble single-walled carbon nanotubes (Ap-SWNTs) loaded with doxorubicin (Dox), Dox/Ap-SWNTs, were synthesized for challenging the MDR of K562 human leukemia cells. The resulting Ap-SWNTs could not only specifically recognize the multidrug resistant human leukemia cells (K562R), but also demonstrate the effective loading and controllable release performance for Dox toward the target K562R cells by exposing to near-infrared radiation (NIR). The recognition capability of Ap-SWNTs toward the K562R cells was confirmed by flow cytometry (FCM) and confocal laser scanning microscopy (CLSM). The binding affinity of Ap-SWNTs toward drug-resistant K562R cells was *ca.* 23-fold higher than that toward drug-sensitive K562S cells. Additionally, CLSM indicated that Ap-SWNTs could specifically localize on the cell membrane of K562R cells and the fluorescence of Dox in K562R cells could be significantly enhanced after the employment of Ap-SWNTs as carrier. Moreover, the composite of Dox and Ap-SWNTs (Dox/Ap-SWNTs) expressed 2.4-fold higher cytotoxicity and showed the significant cell proliferation suppression toward K562R leukemia cells ($p < 0.05$) as compared with free Dox which is popularly employed in clinic trials. These results suggest that the Ap-SWNTs are the promising drug delivery vehicle for overcoming the MDR induced by the overexpression of P-gp on cell membrane. Ap-SWNTs loaded with drug molecules could be used to suppress the proliferation of multidrug resistant cells, destroy the tumor stem cells, and inhibit the metastasis of tumor.

KEYWORDS: multidrug resistance · leukemia cell · drug delivery · carbon nanotubes · doxorubicin

Multidrug resistance (MDR) remains the major obstacle for successful cancer chemotherapy.[1] The mechanisms associated with MDR in cancer have been widely explored.[2,3] The chemotherapy-induced up-regulation of P-glycoprotein (P-gp), a broad-specificity trans-membrane efflux pump that functions as an energy dependent drug efflux pump for a wide variety of substrates,[4] is considered the major event in establishment of MDR in cancer cells.[5] The MDR caused by P-gp frequently exists in the residual tumor cells after chemotherapy and the tumor stem cells inducing the tumor metastasis.[6−8] Overcoming the increased efflux phenomenon, the consequence of the overexpression of multidrug resistance-associated proteins, is the significant challenge for cancer chemotherapy.[9,10] The strategies such as using the inhibitors of drug efflux pump, drug analogues to circumvent the efflux by P-gp, and targeted drug delivery systems have been attempted to overcome the multidrug resistance of cancer cells.[11]

Targeted drug delivery[12,13] is the effective strategy to provide the therapeutic concentrations of anticancer drugs at the targeted cancer cells rather than the noncancerous cells by a variety of functionalized drug carriers, which thus improves the therapeutic efficacy for targeted tissues and reduces the side effects for nontargeted tissues. The efficient delivery, the preservation of drug-molecular bioactivity, and desirable loading and release kinetics of drug molecules toward targets are the driving forces in the design of a targeted drug delivery system.[14,15] Nanoparticle-assisted drug delivery systems could enhance the water-solubility, the circulation time, and the intracellular uptake and preserve the metabolic stability of drugs in cancer cells, while avoiding toxicity in normal cells *via* both passive and active targeting strategies.[16−18]

The carbon nanotubes (CNTs), particularly the functionalized water-soluble CNTs, were suggested to be biocompatible and nontoxic at the cellular level. However, the conclusions on cytotoxicities of CNTs were kind of controversial due to the application of different cytotoxicity assays, the use of CNTs with or without surface modifications and the residual heavy metals in CNTs. It has been reported that the popular applied

*Address correspondence to hanfazou@dicp.ac.cn, wurenan@dicp.ac.cn.

Received for review August 30, 2009 and accepted February 04, 2010.

Published online February 11, 2010. 10.1021/nn9011225

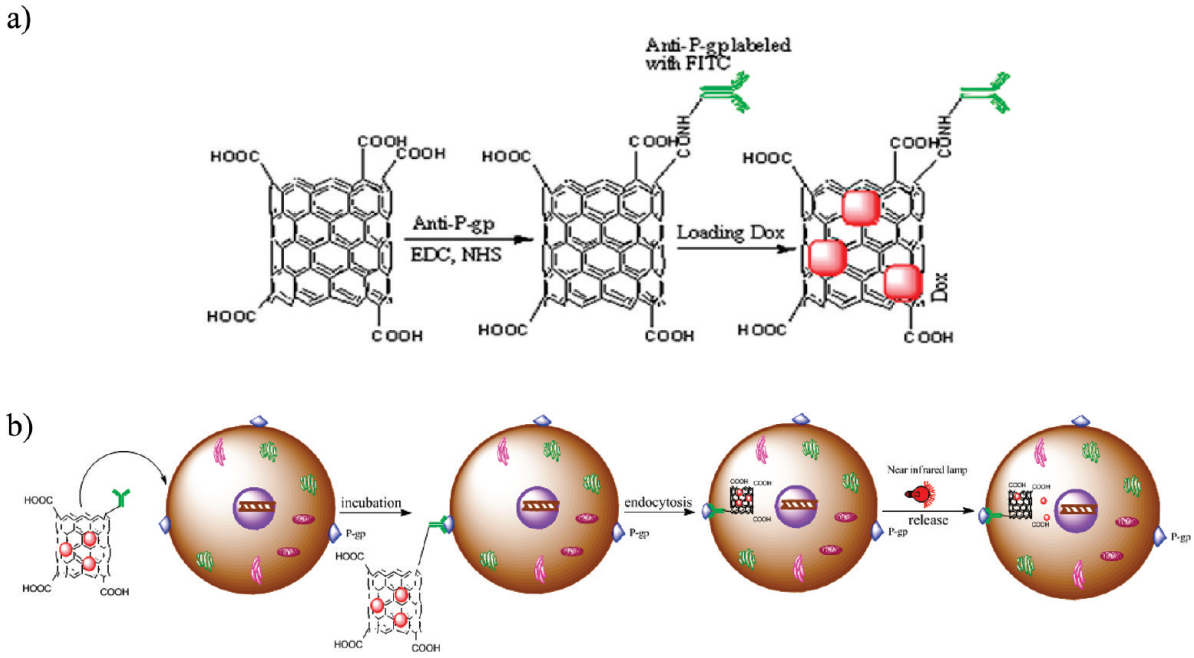

Figure 1. Schematic procedure of utilizing Ap-SWNTs as the targeted Dox-deliver including (a) the synthesis of Ap-SWNTs and loading of Dox, (b) targeting of Ap-SWNTs to membrane P-gp of K562R cells and controllable release of Dox under exposure of NIR.

MTT assay was not appropriate for the test of cytotoxicity induced by CNTs;[19] the crude CNTs were often approved to be cytotoxic rather than the water-soluble functionalized CNTs;[20] and also, the residual heavy metals in CNTs have been confirmed to induce the cytotoxicity.[21] Actually, the functionalized CNTs, which possess excellent biocompatibility and have no residual heavy metals, have been suggested to be nontoxic at cellular level,[22,23] especially for single-walled carbon nanotubes (SWNTs).[24−26] Recently, the functionalized SWNTs have been applied as the molecular carriers for a variety of biomolecules including proteins,[27−29] DNA,[30,31] and RNA[32−34] because of the associated effective endocytosis of CNTs by living cells.[31,35,36]

In our previous work, we have demonstrated the uptakes of water-soluble oxidized carbon nanotubes (o-CNTs) into yeast and human leukemia cells,[37,38] and the effective intracellular uptake of rhodamine 123 (a substrate of P-gp[39]) to the human leukemia cells of K562 by rhodamine 123-loaded o-SWNTs.[40] Interestingly, the intracellular uptakes of rhodamine 123 were enhanced in both the multidrug resistant (K562R) and drug-sensitive (K562S) human leukemia cells, and showed no significant differences in both cell types when the o-SWNTs were used as the carrier of rhodamine 123. That hinted at the potential advantage of o-SWNTs in overcoming the multidrug resistance by circumventing the drug-efflux mechanism of MDR cancer cells. For further achieving the specific delivery of drugs toward the MDR human leukemia cells (K562R) and lowering the concentration of anticancer drugs in normal cells, herein, the anti-P-gp antibody functionalized o-SWNTs (Ap-SWNTs) were prepared for pursuing the targeted drug delivery of doxorubicin (Dox) to the P-gp overexpressed MDR human leukemia cells of K562R. The Ap-SWNTs possess the specificity toward the MDR human leukemia cells by recognizing the overexpressed P-glycoprotein on cell membrane. And, moreover, the Dox could be conveniently loaded on Ap-SWNTs *via* the physical adsorption ($\pi-\pi$ stacking interaction) and could be released controllably into the target cells under the exposure of near-infrared radiation (NIR). The obtained results from this work strongly suggest the promising potential of Ap-SWNTs in overcoming the MDR of human leukemia cells.

RESULTS

Characterization of Ap-SWNTs. The purpose of this work is to challenge the multidrug resistance of human leukemia K562R cells by recognizing the membrane P-gp of the leukemia cells using the P-gp antibody (anti-P-gp) functionalized water-soluble carbon nanotubes, where the anti-P-gp is covalently bonded onto the oxidized single-walled carbon nanotubes (o-SWNTs) *via* a diimide-activated amidation reaction. Figure 1 shows the schematic procedure of the preparation of Ap-SWNTs, the physical loading of Dox on Ap-SWNTs, the targeting of Ap-SWNTs to MDR cells, and the release of Dox to the target cell under the exposure of near-infrared radiation (NIR). For the preparation of Ap-SWNTs, the SWNTs were first oxidized by the mixture of HNO_3 and H_2SO_4 to generate the carboxylic groups (−COOH) on the SWNTs, and then activated by 1-(3-dimethylaminopropyl)-3-ethylcarbodiimide hydrochloride (EDC) and *N*-hydroxysuccinimide (NHS). After that, the activated SWNTs undergo nucleophilic substitution reaction with

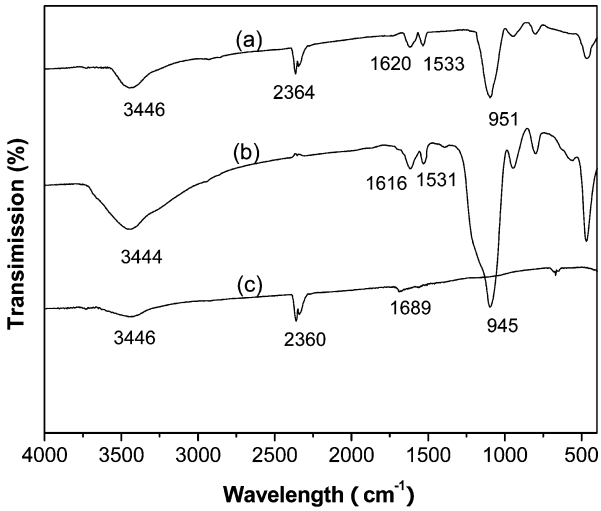

Figure 2. Infrared (IR) spectra of (a) Ap-SWNTs, (b) anti-P-gp, and (c) o-SWNTs. The anti-P-gp antibody is characterized by three IR absorption bands of 945, 1616, 1531, and 3444 cm^{-1} (see spectrum b), which represent the typical absorption bands of glycosidic bonds, amide I, amide II, and free amino groups of protein molecules, respectively. The formation of Ap-SWNTs could be confirmed by the shifted absorption bands of glycosidic bonds, amide I, amide II, and free amino groups at 951, 1620, 1533, and 3446 cm^{-1} (see spectrum a).

the amine groups on the antibody of P-gp labeled with FITC, resulting in the formation of a peptide bond between the o-SWNTs and anti-P-gp proteins. Thus the anti-P-gp immobilized water-soluble carbon nanotubes (Ap-SWNTs) were synthesized. After that, the Dox was physically adsorbed on the Ap-SWNTs *via* the $\pi-\pi$ stacking interaction, and delivered to the MDR human leukemia cells of K562R by the Dox-loaded Ap-SWNTs (Dox/Ap-SWNTs).

For further investigating the immobilization of anti-P-gp antibody on o-SWNTs, the infrared (IR) spectroscopy was applied for the characterization of Ap-SWNTs, anti-P-gp, and o-SWNTs. The obtained IR spectra of Ap-SWNTs, anti-P-gp and o-SWNTs are presented in Figure 2 spectra a, b, c, respectively, with the IR region from 4000 to 400 cm^{-1}. As shown in Figure 2c, the bands at 3448 and 1689 cm^{-1} are corresponding to the typical stretching vibration of O−H and −C═O[41] on carbon nanotubes due to the oxidization of HNO_3 and H_2SO_4. As for anti-P-gp, there are three IR absorption bands at 1616, 1531, and 3444 cm^{-1} (Figure 2b), which are the typical IR bands corresponding to the amide I, amide II, and free amino groups of protein molecules, respectively.[42] After the reaction of anti-P-gp with o-SWNTs, the three typical IR absorption bands of 1616, 1531, and 3444 cm^{-1} for anti-P-gp are shifted to 1620, 1533, and 3446 cm^{-1} (Figure 2a), respectively, because of the covalent bonding of anti-P-gp on the o-SWNTs. Additionally, the bands at 2360 and 945 cm^{-1} are the typical IR bands of CO_2 likely adsorbed on o-SWNTs and the glycosidic bonds of anti-P-gp molecules, respectively. After the conjugation of anti-P-gp with o-SWNTs, both above bands are respectively shifted to 2364 and 951 cm^{-1}, accordingly.

The Loading and Release Performance of Ap-SWNTs for Dox. The *in vitro* loading and release performance are the very important characters for a drug delivery system. The Ap-SWNTs are expected to have the high loading capacity for Dox because of the high surface-to-volume ratio of carbon nanotubes. The *in vitro* loading experiment for Dox on Ap-SWNTs was carried out by dissolving 200 μg of Ap-SWNTs and 100 μg of Dox in 2 mL of PBS buffer solution with stirring at 25°c for 1 h. By filtering the resultant PBS buffer solution through a 0.45 μm filter, followed by the measurement of Dox concentration in filtrate with a Hitachi F-2500 fluorescence spectrophotometer (FS) (λ_{ex}, 488 nm; λ_{em}, 580 nm), the loading of Dox on Ap-SWNTs was estimated by the concentration difference of Dox between the original PBS buffer solution and the filtrate. The concen-

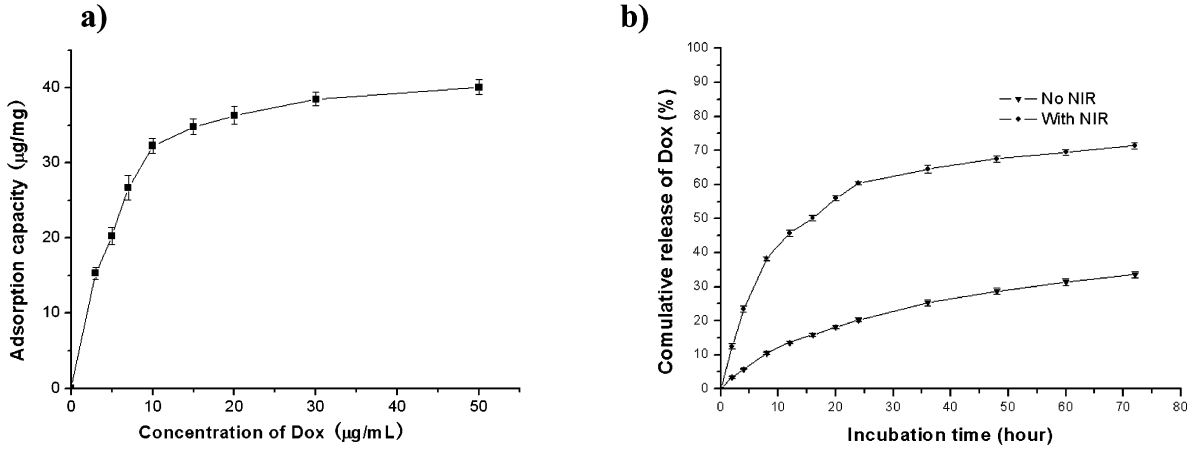

Figure 3. (a) Adsorption isotherm of Dox on Ap-SWNTs and (b) in vitro release profiles of Dox from Ap-SWNTs. The adsorption isotherm indicates excellent loading capacity of Ap-SWNTs as the drug deliverer; the saturated adsorption capacity for Dox could reach 40 μg/mg (panel a). The release profiles include the spontaneous release curve and the controlled release curve under near-infrared radiation. The release of Dox from Ap-SWNTs can be controlled by the near-infrared radiation (NIR), which is significantly enhanced as compared to that without the NIR.

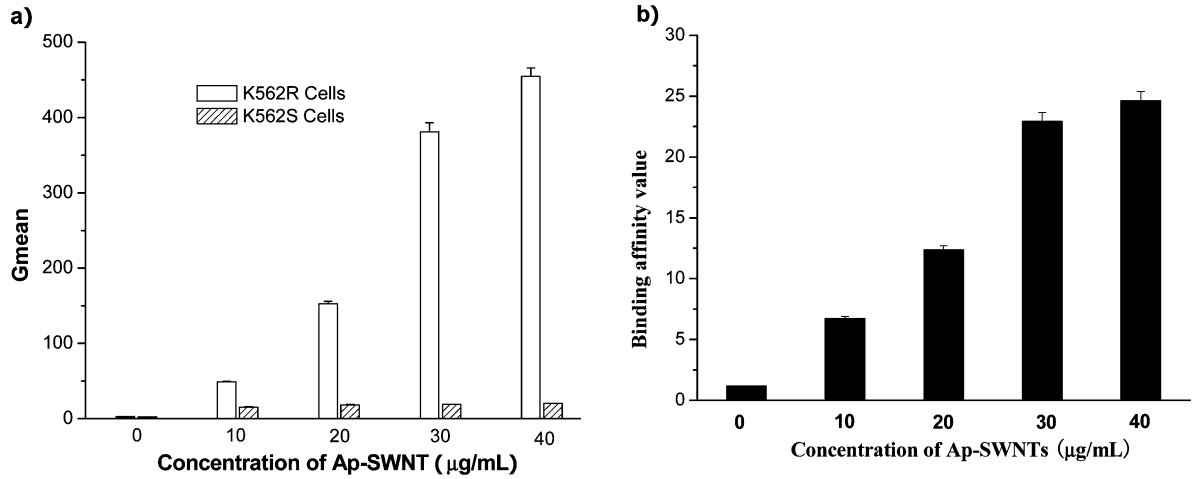

Figure 4. (a) The G_{mean} value of Ap-SWNTs in K562R and K562S cells by flow cytometry analysis. (b) The binding affinity values of Ap-SWNTs for K562R *vs* K562S cells. These flow cytometric results indicate good specific affinity of Ap-SWNTs to P-gp overexpressed multidrug resistant K562R leukemia cells.

trations of Dox ranged from 0 to 50 μg/mL in the PBS buffer solutions. Figure 3a shows the resulting adsorption isotherm of Dox on Ap-SWNTs, which can be expressed with a Langmuir adsorption equation of $q = (79.89C_e)/(1 + 1.75C_e)$ ($R^2 = 0.9898$), where q and C_e represent the adsorption capacity and the equilibrium concentration of Dox on Ap-SWNTs, respectively; R^2 is used to assess the fitting degree. This Langmuir isotherm adsorption approximation indicates the monomolecular adsorption of Dox on Ap-SWNTs. It also can be seen that the Ap-SWNTs have the maximum loading capacity of *ca*. 40 μg/mg for Dox.

On the other hand, the *in vitro* release of Dox from Ap-SWNTs were examined. At first, 1 mg of Ap-SWNTs was dissolved in 2 mL of 100 μg/mL of Dox solution and stirred for 1 h to completely adsorb Dox. After that, the mixture was filtered and the content of Dox in filtrate was measured by FS, and the amount of Dox loaded on Ap-SWNTs was the difference of Dox in the original PBS solution over that in the filtrate. Then Dox/Ap-SWNTs composite together with the filter paper were dispersed into 2 mL of PBS solution and placed into a filter bag. After the filter bag was immerged into 10 mL of PBS solution in a glass bottle, the bottle was exposed to a Philips PAR 38 infrared lamp (Philips, Eindhoven, Netherlands) and stirred for 5 min (see Supporting Information, Figure S-2a), and the liquid level is *ca*. 15 cm away from the lamp. Then, the bottle was placed into a shaker and dialyzed at 25 °C with a rate of 100 rpm/min. Within a 2-h dialysis period, a 5 min near-infrared radiation (0.2 W/cm^2) generated by a near-infrared lamp was applied on the dialysis device for three times during each 35 min interval (see Supporting Information, Figure S-2b). Besides, the dialyzate was refreshed every 2 h, and the concentration of Dox in dialyzate was detected by FS. For comparison, the *in vitro* release experiment with the absence of near-infrared radiation during dialysis was performed under the same dialysis condition. The accumulative release value of Dox could be calculated on the basis of the formula described as $R = \sum C_i/C_{total} \times 100$, where R represents the accumulative release value, C_i is the content of Dox in dialyzate during each 2-h dialysis period, and C_{total} is the adsorption capacity of Dox. The obtained results are shown in Figure 3b, it is observed that the release of Dox from Ap-SWNTs is slow with the absence of the near-infrared radiation. Only 20% of Dox is released from Ap-SWNTs within 24 h without the near-infrared radiation. Whereas, the Dox release could be significantly enhanced (nearly 60% of Dox is released from Ap-SWNTs within 24 h) when the Ap-SWNTs are exposed to the near-infrared radiation during dialysis.

The Recognition Capability of Ap-SWNTs toward the MDR K562R Cells. The primary goal of this work is to challenge the multidrug resistance of human leukemia cells by the targeted drug delivery of Dox carried on Ap-SWNTs. The recognition capability of Ap-SWNTs toward the MDR K562R cells is the essential property for this targeted drug delivery system. For evaluating this recognition capability, K562S and K562R human leukemia cells (*ca*. 1×10^7) were incubated in media containing 0, 10, 20, 30, and 40 μg/mL of Ap-SWNTs for 30 min. Since the anti-P-gp antibody immobilized on o-SWNTs has been labeled by FITC, the uptake of Ap-SWNTs by the K562 cells could be determined by flow cytometry. Figure 4a shows the geometric mean florescence intensity (G_{mean}) values of Ap-SWNTs in K562S and K562R cells treated by Ap-SWNTs at different concentrations (histograms shown in Supporting Information, Figure S-4). The expression of P-gp in K562R cells was nearly 458-times higher than K562S cells (see Supporting Information, Figure S-3). So the higher G_{mean} values were observed for K562R cells as compared to K562S cells at each concentration of Ap-SWNTs. To evaluate the targeted capability of Ap-SWNTs, a binding affinity value (A) was defined as: $A = G_{mean_{K562R}}/G_{mean_{K562S}}$. The obtained

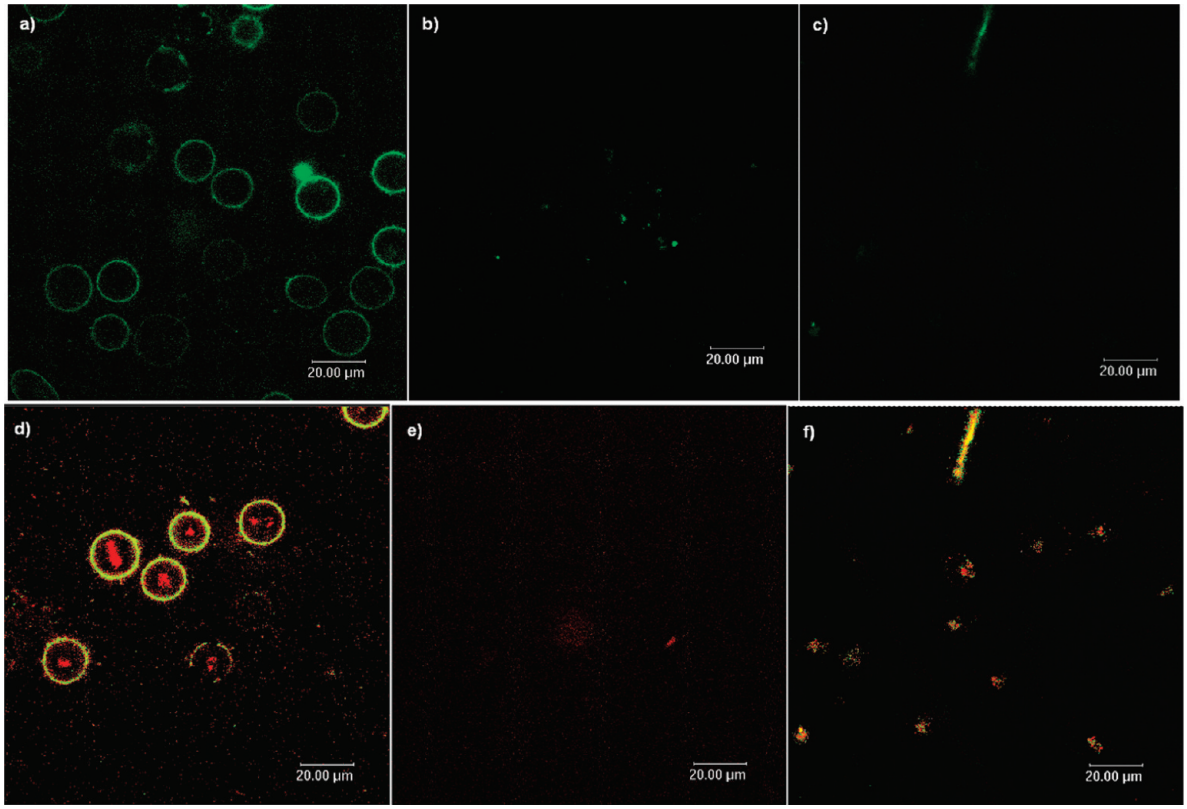

Figure 5. Confocal microscopy images of (a) K562R cells treated by Ap-SWNTs, (b) K562S cells treated by Ap-SWNTs, (c) K562R cells treated by HSA-SWNTs, (d) K562R cells treated by Dox/Ap-SWNTs, (e) K562R cells treated by free Dox, and (f) K562R cells treated by Dox/HSA-SWNTs. Green spots represent Ap-SWNTs or HSA-SWNTs, and red spots represent Dox under confocal microscopy. Apparently, Ap-SWNTs are located on the cell membrane of K562R cells (panel a) due to the overexpression of P-gp as comparing to drug-sensitive K562S cells (panel b), and the dim green fluorescence indicates that HSA-SWNTs do not have the specific targeted capability (panel c). Also the fluorescence of Dox delivered by Ap-SWNTs is stronger than free Dox and HSA-SWNTs as comparing panel d to panel f.

binding affinity values are shown in Figure 4b. It could be found that the binding affinity values were in a dose-dependent manner as the concentration of Ap-SWNTs changed from low to high level. The binding affinities of Ap-SWNTs for K562R cells is *ca.* 23-fold higher than that in K562S cells while there is 30 μg/mL of Ap-SWNTs in culture media.

For further studying the intracellular distribution of Ap-SWNTs in the MDR cells, both K562R and K562S cells (*ca.* 1×10^7) were incubated in media containing 30 μg/mL of Ap-SWNTs for 30 min. Because of the presence of FITC on Ap-SWNTs, the Ap-SWNTs attached on cells could be observed by confocal laser scanning microscopy (CLSM). Figure 5 panels a and b show the obtained fluorescent images of K562R and K562S cells. As can be seen, the Ap-SWNTs were clearly localized on the cell membrane of K562R cells. However, there was no Ap-SWNTs observed on cell membrane for K562S cells but in the cytoplasm. Furthermore, K562R cells were incubated with the human serum albumin (labeled with FITC) functionalized SWNTs (HSA-SWNTs, 30 μg/mL for 30 min) and observed under CLSM. The obtained image is shown in Figure 5c, where the fluorescence of HSA-SWNTs in K562R cells is dim. All of the three images (the corresponding bright field images and single channel images shown in Supporting Information Figures S-5a−c,i,g) demonstrate the specific targeted capability of Ap-SWNTs very well.

For a targeted drug delivery system, the successful delivery of drugs into the targeted cells is the terminal purpose. To evaluate the delivery of Dox by Ap-SWNTs, K562R cells (*ca.* 1×10^7) were incubated with media containing Dox/Ap-SWNTs composites (20 μg/mL of Dox, 30 μg/mL of Ap-SWNTs), free Dox (20 μg/mL of Dox), and Dox/HSA-SWNTs (20 μg/mL of Dox, 30 μg/mL of HSA-SWNTs), respectively, at 37 °C for 8 h. During the incubation, a 5-min near-infrared radiation was periodically applied on these cell samples for three times to enhance the release of Dox to cells from Ap-SWNTs. The intracellular Dox delivered by Ap-SWNTs was monitored by CLSM in this work. The obtained CLSM images are illustrated in Figure 5d−f (the corresponding bright field images and single channel images shown in Supporting Information, Figure S-5d−i), where the red and green fluorescence represent the Dox and Ap-SWNTs, respectively. Figure 5d shows that the fluorescence of Dox in cells is rather bright, which indicates more Dox was delivered into K562R cells by Ap-SWNTs. In contrast, inconspicuous red Dox spots appeared if the K562R cells were incubated with free Dox (Figure

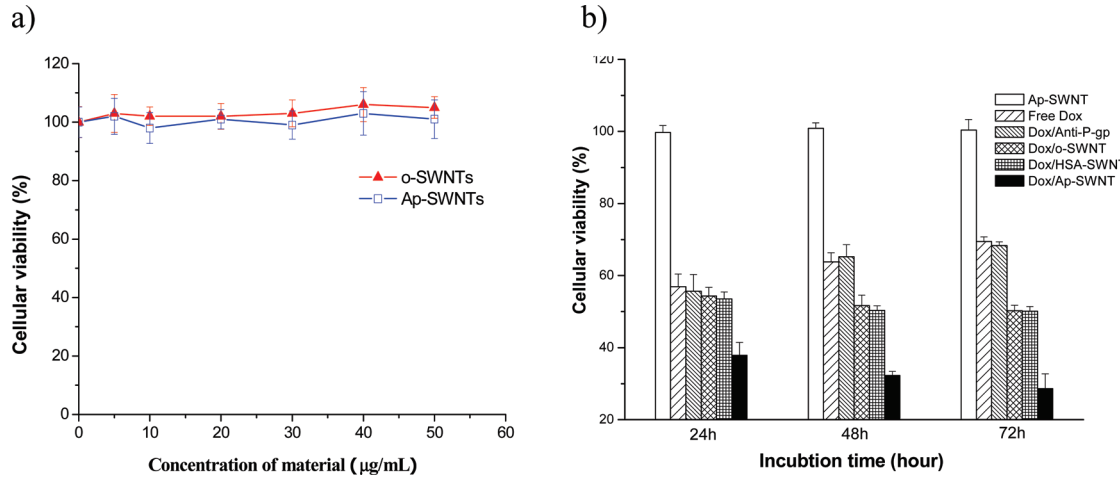

Figure 6. (a) The viability of K562R cells treated by o-SWNTs and Ap-SWNTs; (b) the viability of K562R cells treated by Ap-SWNTs, free Dox, Dox/anti-P-gp, Dox/o-SWNTs, Dox/HSA-SWNTs, and Dox/Ap-SWNTs with 24, 48, and 72 h incubation. The cytotoxicity assay was tested on 96-well plate. All of the four agents contained same concentration of Dox in culture media, which was *ca.* 5 μg/mL. The results indicate that Dox/anti-P-gp has similar cytotoxicity with free Dox, while Dox/HSA-SWNTs and Dox/o-SWNTs express higher cytotoxicity than free Dox and Dox/Ap-SWNTs possess the highest cytotoxicity. Nearly 242% enhancement of cytotoxicity was observed after 72-h incubation, and it indicates that the cytotoxicity of Dox/Ap-SWNTs is time-dependent.

5e), whereas HSA-SWNTs exhibit a medium level in the delivery of Dox into K562R cells (Figure 5f).

The Intracellular Pathway of Ap-SWNTs. It is essential to study the intracellular mechanism of Ap-SWNTs as a novel drug deliverer for its further clinical applications. There are two possible mechanisms involved in the intracellular uptake of carbon nanotubes by cells, namely the penetration and the endocytosis. The endocytosis mechanism is known as an energy-dependent uptake for various extracellular materials, which can be suppressed by incubating cells at low temperature, whereas the penetration mechanism performs in an energy-independent manner. For determining the uptake behavior of Ap-SWNTs by K562R cells, the cells were incubated with Ap-SWNTs at 4 and 37 °C. The intracellular uptakes of Ap-SWNTs at different incubation temperature were monitored by flow cytometry (FCM), and we find that the intracellular uptake of Ap-SWNTs by K562R cells at 37 °C is 3.8-times higher than that at 4 °C (see Supporting Information, Figure S-5). Thus it could be concluded that Ap-SWNTs enter into leukemia cells *via* endocytosis. As shown in Figure 5a, the fluorescent Ap-SWNTs could be clearly observed on the cell membrane of K562R cells by CLSM due to the specific targeting of Ap-SWNTs to K562R cells. We assume that the Ap-SWNTs are initially conjugated with the site of P-gp on the outside of membrane and then endocytosed by K562R cells and localized on the inside of membrane.

Dox-Induced Cytotoxicity by Ap-SWNT. During chemotherapy, the residual tumor cells and tumor stem cells are hard to clear up, which directly induces the failure of chemotherapy. In this study, the new drug vehicle, Ap-SWNTs, are designed to assist the antitumor agents to eliminate the multidrug resistant cells, and the cytotoxicity of Ap-SWNTs loaded with Dox against the multidrug resistant cells was examined.

Before that, the biological safety of Ap-SWNTs along with o-SWNTs was evaluated. Namely, 100 μL of K562R cells (1×10^4) were seeded on a 96-well plate and cultured for 24 h. Followed by adding 100 μL of Ap-SWNTs or o-SWNTs solutions (0−100 μg/mL of material in medium) and being incubated for 48 h, the cell viabilities were tested on the 96-well plate *via* the WST-1 assay. As shown in Figure 6a, the cell viabilities of K562R cells remain unaffected as the concentrations of o-SWNTs and Ap-SWNTs varied from 0 to 50 μg/mL. On the basis of the material biosafety investigation of Ap-SWNTs, the Dox-induced cellular cytotoxicities were carried out by incubating K562R cells with free Dox, Ap-SWNTs, Dox/HSA-SWNTs, Dox/anti-P-gp, Dox/o-SWNTs, and Dox/Ap-SWNTs on a 96-well plate with equivalent concentrations of Dox, anti-P-gp, and functionalized SWNTs (Ap-SWNTs, o-SWNTs, and HSA-SWNTs) at 5, 0.06, and 30 μg/mL in media. After the K562R cells (1×10^4 cells/100 μL of media/well) were seeded and incubated for 24 h, 100 μL of media containing all of the above agents was added into each well and the cell samples were sequentially incubated for 6 h. After that, the culture media were replaced with fresh ones and the cell samples were incubated for 24, 48, and 72 h, respectively. While, for releasing the Dox from the composites, a 5 min near-infrared radiation was applied on the cell samples every 8 h during the incubation periods. The Dox-induced cytotoxicities for all these agents are illustrated in Figure 6b. The cellular viabilities of K562R cells incubated with Ap-SWNTs remained at *ca.* 100%, which indicated the insignifi-

cant effect to the survival of K562R cells for Ap-SWNTs even under the exposure of NIR ($n = 9$, $p > 0.123$, compared to 100%). Free Dox and Dox/anti-P-gp composite demonstrate similar cytotoxicities to K562R cells, and the growth of K562R cells would gradually bloom as the increase of the incubation time ($n = 9$). However, by conjugating Dox with o-SWNTs, HSA-SWNTs, or Ap-SWNTs, the cytotoxicity of Dox toward K562R cells is correspondingly enhanced. The Dox/Ap-SWNTs composite demonstrates the predominant cytotoxicity (*ca.* 2.4-fold higher than that induced by free Dox) toward K562R cells as compared to the other agents ($n = 9$, $p < 0.05$).

DISCUSSION

Chemotherapy is an important cure strategy for cancer patients. However, the multidrug resistance (MDR), which broadly exists in residual tumor cells after chemotherapy and tumor stem cells, has become the major obstacle for cancer therapy. The up-regulated P-glycoprotein that increases the drug-efflux is considered the major event for the establishment of MDR in cancer cells. The P-gp blockers and targeted drug deliverers are the major approaches for MDR; however, the former is hard to succeed *in vivo*.[43] While the targeted drug deliverers, especially the targeted nanoparticles (NPs), have attracted much attention due to the enhanced permeability and retention (EPR) effects in tumors. There are three classes of targeted deliverers including lipid nanocapsules,[44] polymer NPs,[45] and inorganic NPs. Among them, lipid nanocapsules and polymer NPs have outstanding advantages in biocompatibility and are widely studied, but the instability and low loading capacity are the major problems. On the contrary, inorganic NPs as targeted deliverers for MDR possess wonderful stability but inferior biocompatibility. So far, only three kinds of inorganic nanoparticles including ZnO,[46] gold,[47] and Fe_3O_4 NPs[48] have been studied as deliverers for MDR, though the further desirable functionalization of these nanomaterials seems a problem still. Nonetheless, the preservation of the biological activity for delivered drugs, the desirable loading capacity, and controllable release of drug molecules and the specific targeting performance are the driving forces for the design of targeted drug delivery system. In the past years, carbon nanotubes, due to their inherent properties, had been employed in the intracellular delivery of macrobiological molecules.[34,35] In this work, we employed anti-P-gp antibody functionalized SWNTs (Ap-SWNTs) as a targeted drug deliverer for overcoming the MDR of human leukemia cells (K562R) for the first time.

Here, the antibody against P-glycoprotein (anti-P-gp) is immobilized on the o-SWNTs *via* a diimide-activated amidation approach in aqueous MES buffer, where the biological activity of antibody could be well preserved. Additionally, the oxidization of carbon nanotube mainly occurs at the end of carbon nanotube, so the remaining surface of carbon nanotube could still be used for the loading of drugs (*e.g.*, Dox in this work) even after the coupling with an antibody. The obtained loading capacity for Dox on Ap-SWNTs is *ca.* 40 μg/mg, which is attributed to the remaining high surface area of carbon nanotube itself. This high loading capacity indicates that the carbon nanotube based drug carriers could provide desirable loading performance for Dox. In fact, many of the small molecular anticancer drugs could be physically adsorbed on carbon nanotubes *via* the hydrophobic interactions of drugs on carbon nanotube. Comparing to the covalent bonding of small molecules on carbon nanotubes,[49−52] the physical adsorption of drugs on Ap-SWNTs would maximally preserve the molecular integrity due to the avoid of chemical reactions between drugs and carbon nanotubes. Additionally, the carbon nanotube is the good energy absorption material for laser and near-infrared radiation.[30,53] While exposed under NIR, Ap-SWNTs will adsorb the energy from NIR, which would consequently improve the release of Dox from Ap-SWNTs as the endothermic process of Dox desorption from SWNTs. We believe that this noncovalent drug-delivery manner is a promising strategy for delivering drugs to different types of cells with the most minimum loss of drug activities along with the controllable release of drugs from carbon nanotubes by near-infrared radiation.

For further demonstrating the suppression of Dox/Ap-SWNTs to the proliferation of the multidrug resistant leukemia cells, the cytotoxicity assay is carried out. As shown in Figure 6b, free Dox and Dox/anti-P-gp have similar cytotoxicity to K562R cells, and the growth of K562R cells would gradually bloom along with longer incubation time. These results implied that free Dox, popularly employed in clinic, is unable to suppress the proliferation of K562R cells, which would lead to the failure of chemotherapy and even the death of patients. Also, anti-P-gp has no influences to the cytotoxicity of Dox. The o-SWNTs, HSA-SWNTs, and Ap-SWNTs all enhance the cytotoxicity of Dox to the multidrug resistant K562R cells, while the prepared Dox/Ap-SWNTs demonstrated the highest cytotoxicity to K562R cells. Most importantly, the cytotoxicity of Dox/Ap-SWNTs was time-dependent; normally, the longer the incubation time was, the greater was the proliferation inhibition of K562R cells. This exciting phenomenon is due to two excellent characters of Ap-SWNTs, one is the prolonged release ability and another is the specific recognition capability. All of the results from FCM, CLSM, and cytotoxicity assays indicate that Dox carried by Ap-SWNTs can be well delivered to multidrug resistant cells, and success-

fully suppress the proliferation of K562R cells. This can be explained as (1) there will be much more Dox in K562R cells as Ap-SWNTs targeted on K562R cells; (2) it is difficult to pump Ap-SWNTs out by P-gp because of the nanosize vehicles rather than the small molecules of Dox; (3) Ap-SWNTs could conjugate with P-gp and there would be huge stereohindrance around the P-gp molecule, which greatly suppressed the out-efflux of Dox by MDR existed cells.

Moreover, the intracellular uptake of Dox in K562R cells incubated with all of the above agents was measured by capillary electrophoresis coupled with laser-induced fluorescence (CE-LIF),[40] and it was found that the obtained results from CE-LIF are accordant with the conclusions from cytotoxicity tests (see Supporting Information SI-3 and Figure S-7). Finally, the apoptosis test for K562R cells treated with Dox/Ap-SWNTs was carried out on FCM. Annexin V (labeled with FITC) coupled with PI are the popular agents for the test of apoptosis on FCM.[54] After incubation with the agents, the early apoptosis cells would conjugate with Annexin V, the advanced apoptosis cells would conjugate with both Annexin V and PI and the necrotic cells would conjugate only with PI. The obtained results (see Supporting Information SI-4 and Figure S-8) indicate that Dox/Ap-SWNTs would trigger the apoptosis pathway of K562R cells and suppress the proliferation, which is similar with Dox. And it implies that the deliverer, Ap-SWNTs, do not influence the apoptotic mechanism of the carried drugs. Thus, Ap-SWNTs may be the good carriers for delivering drug molecules into cells, which are not only an efficient strategy for overcoming the pumping-out function of P-gp, but also possess the prolonged drug release ability.

CONCLUSIONS

For the first time, for the best of our knowledge, an anti-P-gp antibody functionalized single-walled carbon nanotubes (Ap-SWNTs) as targeted drug deliverer for MDR were synthesized. The prepared novel drug-vehicle demonstrated the advantages in biocompatibility, controlled release ability, and targeted capability in cellular level to overcome the MDR of human leukemia cells. In this work, the P-gp antibody functionalized carbon nanotubes (Ap-SWNTs) were synthesized *via* the biocompatible diimide-activated amidation reaction between the antibody and the water-soluble oxidized single-walled carbon nanotube. By taking advantage of the specific affinity of the immobilized antibody to the membrane P-gp overexpressed in the multidrug resistant human leukemia cells, the obtained Ap-SWNTs were thus applied in the targeted drug delivery of doxorubicin (Dox) to the multidrug resistant leukemia (K562R) cells. Additionally, the anticancer drug of Dox was loaded on the surface of Ap-SWNTs *via* the noncovalent physical adsorption, so it could be controllably released into target cells *via* the exposure of near-infrared radiation (NIR). Moreover, the induced cytotoxicity of Dox to the multidrug resistance leukemia cells (K562R) has been significantly enhanced by loading Dox on Ap-SWNTs. It can be concluded that the Ap-SWNTs are a promising vehicle for the targeted drug delivery of Dox to the multidrug resistance during cancer therapy.

EXPERIMENTAL SECTION

Reagents and Materials. P-glycoprotein antibody (anti-P-gp) labeled with FITC was purchased from BD Biosciences (Franklin Lakes, NJ); doxorubicin was purchased from Sigma-Aldrich (St. Louis, MO); 2-(4-Iodophenyl)-3-(4-nitrophenyl)-5-(2, 4-disulfophenyl)-2H-tetrazolium, monosodium salt (WST-1) and 1-methoxy-5-methylphenazinium methylsulfate (PMS) were purchased from Dojindo laboratory (Kumamoto, Japan); 1-(3-dimethylaminopropyl)-3-ethylcarbodiimide hydrochloride (EDC) and *N*-hydroxysuccinimide (NHS) were purchased from Pierce (Pierce, IL); human serum albumin was purchased from Sigma-Aldrich (St. Louis, MO); single-walled carbon nanotube (SWNTs) were purchased from Sino-nano Company (Beijing, China), and treated by the mixture of concentrated HNO_3/H_2SO_4 (1:3 v/v) at 120 °C for 30 min under reflux with stirring to produce the oxidized single-walled carbon nanotubes (o-SWNTs).[55] The obtained o-SWNTs were further redispersed in water, centrifuged at 10000*g* for 30 min to remove the water immiscible carbon nanotubes or other residuals, lyophilized to dryness at room temperature, and stored at 4 °C before use.

Cell Culture. The multidrug resistance (K562R) and drug-sensitive (K562S) human leukemia cells were obtained from the Institute of Blood, Chinese Academy of Medical Sciences (Tianjin, China), which were seeded initially at a density of 1.0×10^4 cells/mL and cultured in 75-cm^2 vented culture flasks at 37 °C with RPMI-1640 medium containing 10% calf serum in 5% carbon dioxide atmosphere, and split every 2−3 days.

The Preparation of anti-P-gp Functionalized Carbon Nanotubes (Ap-SWNTs). The AP-SWNTs were prepared by covalently bonding the anti-P-gp antibody on the o-SWNTs *via* the diimide-activated amidation process as described in the literature.[56] The scheme for this preparation is presented in Figure 1. Briefly, 5 mg of the water-soluble o-SWNTs, 30 mg of 1-(3-dimethylaminopropyl)-3-ethylcarbodiimide hydrochloride (EDC), and 300 mg of *N*-hydroxysuccinimide (NHS) were added in a 10 mL aqueous buffer solution of 2-(4-morpholino)ethanesulfonic acid (MES) (50 mM, pH = 6.0), mixed, and shaken in a reciprocating shaker at room temperature for 2 h. After that, the resultant SWNTs were filtered through a 0.45 μm filter, fully rinsed with 50 mM MES buffer, and redissolved in a 10 mL MES buffer solution (50 mM, pH = 6.0). Subsequently, 1 mL of anti-P-gp solution (0.025 mg/mL) was added, and the mixture was shaken at room temperature for 2 h. This was followed by a filtration through 0.45 μm filter and a consecutive rinse with 2 mL of NaCl solution (0.1 M) until there was no antibody detected in the filtrate by a Hitachi F-2500 fluorescence spectrophotometer (FS) (Pleasanton, CA, USA) with excitation at 488 and emission at 533 nm. Finally, the resulting Ap-SWNTs were collected, lyophilized to dryness, and stored at 4 °C before use (TEM image of Ap-SWNTs shown in Supporting Information, Figure S-1). Additionally, human serum albumin (HSA) labeled with FITC was conjugated with o-SWNTs by the same procedure and applied as a control.

Flow Cytometry and Confocal Laser Scanning Microscopy Analysis. The flow cytometry analysis was carried out on a FACS Vantage SE flow cytometer from BD (Franklin Lakes, NJ) with Ar-ion (λ = 488 nm) excitation. The flow cytometric data were collected and pro-

cessed using WinMDI 2.9 Software (TSRI, La Jolla, CA). The confocal laser scanning microscopy analysis was performed by a TCS-SP2 confocal laser scanning microscope (Leica, Wetzlar, Germany) with an 80× objective. Before these analyses, the obtained cell samples (*ca.* 1×10^7) were rinsed with PBS buffer (4 °C) for three times and resuspended in 500 μL of PBS buffer.

Cellular Viability Measurement. The cellular viabilities were measured by a model 550 ELISA reader (BIO-RAD, Hercules, CA) with detection wavelength at 450 nm. K562 cells (1×10^4) were initially seeded in the wells of a 96-well plate and incubated in RPMI 1640 cell culture media under certain incubation conditions as indicated. After the incubation, the media on plate were replaced by 200 μL fresh culture media containing 200 μM WST-1 and 1 μM PMS,[57] and the cells were incubated for additional 3 h before the cellular viability test. All experiments were performed in triplicate and the results were analyzed by SPSS 15.0 software (SPSS, Chicago, IL). One-Way ANOVA and student's *t* test were used to determine the statistical differences. Difference was considered significant for p value <0.05.

Acknowledgment. This work was supported by the National Natural Science Foundation of China (No. 20327002, 20735004), the State Key Basic Research Development Program of China (973 Program) (No. 2005CB522701), the Knowledge Innovation Program of Dalian Institute of Chemical Physics to H. Zou; the National Natural Science Foundation of China (No. 20875089), the National High Technology Research and Development Program of China (863 Program) (No. 2008AA02Z211) and the Hundred Talent Program of the Chinese Academy of Sciences to R. Wu.

Supporting Information Available: TEM images for Ap-SWNTs, the optimization of near-infrared radiation exposure, the targeting capability tests of anti-P-gp and Ap-SWNTs on flow cytometry, bright field and single channel images on confocal microscopy, results of the intracellular uptake pathway of Ap-SWNTs, detection of Dox in K562R cells on capillary electrophoresis, apoptosis assay, and the images of cell samples stained by DAPI. This material is available free of charge *via* the Internet at http://pubs.acs.org.

REFERENCES AND NOTES

1. Clarke, R.; Leonessa, F.; Trock, B. Multidrug Resistance/P-Glycoprotein and Breast Cancer: Review and Metaanalysis. *Semin. Oncol.* **2005**, *32*, 9–15.
2. Krishna, R.; Mayer, L. D. Multidrug Resistance (MDR) in Cancer—Mechanisms, Reversal Using Modulators of MDR and the Role of MDR Modulators in Influencing the Pharmacokinetics of Anticancer Drugs. *Eur. J. Pharm. Sci.* **2000**, *11*, 265–283.
3. Zgurskaya, H. I.; Nikaido, H. Multidrug Resistance Mechanisms: Drug Efflux across Two Membranes. *Mol. Microbiol.* **2000**, *37*, 219–225.
4. Mahon, F. X.; Belloc, F.; Lagarde, V.; Chollet, C.; Moreau-Gaudry, F.; Reiffers, J.; Goldman, J. M.; Melo, J. V. MDR1 Gene Overexpression Confers Resistance to *Imatinib mesylate* in Leukemia Cell Line Models. *Blood* **2003**, *101*, 2368–2373.
5. Li, X.; Li, J. P.; Yuan, H. Y.; Gao, X.; Qu, X. J.; Xu, W. F.; Tang, W. Recent Advances in P-Glycoprotein-Mediated Multidrug Resistance Reversal Mechanisms. *Methods Find. Exp. Clin. Pharmacol.* **2007**, *29*, 607–617.
6. Mizutani, T.; Masuda, M.; Nakai, E.; Furumiya, K.; Togawa, H.; Nakamura, Y.; Kawai, Y.; Nakahira, K.; Shinkai, S.; Takahashi, K. Genuine Functions of P-Glycoprotein (ABCB1). *Curr. Drug Metab.* **2008**, *9*, 167–174.
7. Dingli, D.; Michor, F. Successful Therapy Must Eradicate Cancer Stem Cells. *Stem Cells* **2006**, *24*, 2603–2610.
8. Dean, M.; Fojo, T.; Bates, S. Tumour Stem Cells and Drug Resistance. *Nat. Rev. Cancer* **2005**, *5*, 275–284.
9. Eckstein-Ludwig, U.; Webb, R. J.; Van Goethem, I. D.; East, J. M.; Lee, A. G.; Kimura, M.; O'Neill, P. M.; Bray, P. G.; Ward, S. A.; Krishna, S. Artemisinins Target the SERCA of *Plasmodium falciparum*. *Nature* **2003**, *424*, 957–961.
10. Fiskus, W.; Rao, R.; Fernandez, P.; Herger, B.; Yang, Y.; Chen, J.; Kolhe, R.; Mandawat, A.; Wang, Y.; Joshi, R.; *et al*. Molecular and Biologic Characterization and Drug Sensitivity of Pan-Histone Deacetylase Inhibitor-Resistant Acute Myeloid Leukemia Cells. *Blood* **2008**, *112*, 2896–2905.
11. Yuan, H. Y.; Li, X.; Wu, J. F.; Li, J. P.; Qu, X. J.; Xu, W. F.; Tang, W. Strategies to Overcome or Circumvent P-Glycoprotein Mediated Multidrug Resistance. *Curr. Med. Chem.* **2008**, *15*, 470–476.
12. Vasir, J. K.; Labhasetwar, V. Targeted Drug Delivery in Cancer Therapy. *Technol. Cancer Res. Treat.* **2005**, *4*, 363–374.
13. Spragg, D. D.; Alford, D. R.; Greferath, R.; Larsen, C. E.; Lee, K. D.; Gurtner, G. C.; Cybulsky, M. I.; Tosi, P. F.; Nicolau, C.; Gimbrone, M. A., Jr. Immunotargeting of Liposomes to Activated Vascular Endothelial Cells: A Strategy for Site-Selective Delivery in the Cardiovascular System. *Proc. Natl. Acad. Sci. U.S.A.* **1997**, *94*, 8795–8800.
14. Sharma, A.; Sharma, U. S. Liposomes in Drug Delivery: Progress and Limitations. *Int. J. Pharm.* **1997**, *154*, 123–140.
15. Allen, T. M.; Cullis, P. R. Drug Delivery Systems: Entering the Mainstream. *Science* **2004**, *303*, 1818–1822.
16. Vauthier, C.; Dubernet, C.; Chauvierre, C.; Brigger, I.; Couvreur, P. Drug Delivery to Resistant Tumors: The Potential of Poly(alkyl cyanoacrylate) Nanoparticles. *J. Controlled Release* **2003**, *93*, 151–160.
17. Lacoeuillel, F.; Garcion, E.; Benoit, J. P.; Lamprecht, A. Lipid Nanocapsules for Intracelluar Drug Delivery of Anticancer Drugs. *J. Nanosci. Nanotechnol.* **2007**, *7*, 4612–4617.
18. Xu, P. S.; Van Kirk, E. A.; Zhan, Y. H.; Murdoch, W. J.; Radosz, M.; Shen, Y. Q. Targeted Charge-Reversal Nanoparticles for Nuclear Drug Delivery. *Angew. Chem., Int. Ed.* **2007**, *46*, 4999–5002.
19. Worle-Knirsch, J. M.; Pulskamp, K.; Krug, H. F. Oops They Did It Again! Carbon Nanotubes Hoax Scientists in Viability Assays. *Nano Lett.* **2006**, *6*, 1261–1268.
20. Sargent, L. M.; Shvedova, A. A.; Hubbs, A. F.; Salisbury, J. L.; Benkovic, S. A.; Kashon, M. L.; Lowry, D. T.; Murray, A. R.; Kisin, E. R.; Friend, S.; *et al*. Induction of Aneuploidy by Single-Walled Carbon Nanotubes. *Environ. Mol. Mutagen.* **2009**, *50*, 708–717.
21. Lewinski, N.; Colvin, V.; Drezek, R. Cytotoxicity of Nanoparticles. *Small* **2008**, *4*, 26–49.
22. Chlopek, J.; Czajkowska, B.; Szaraniec, B.; Frackowiak, E.; Szostak, K.; Beguin, F. *In Vitro* Studies of Carbon Nanotubes Biocompatibility. *Carbon* **2006**, *44*, 1106–1111.
23. Lacerda, L.; Bianco, A.; Prato, M.; Kostarelos, K. Carbon Nanotubes as Nanomedicines: From Toxicology to Pharmacology. *Adv. Drug Delivery Rev.* **2006**, *58*, 1460–1470.
24. Lu, Q.; Moore, J. M.; Huang, G.; Mount, A. S.; Rao, A. M.; Larcom, L. L.; Ke, P. C. RNA Polymer Translocation with Single-Walled Carbon Nanotubes. *Nano Lett.* **2004**, *4*, 2473–2477.
25. Kam, N. W. S.; Liu, Z.; Dai, H. J. Functionalization of Carbon Nanotubes *via* Cleavable Disulfide Bonds for Efficient Intracellular Delivery of siRNA and Potent Gene Silencing. *J. Am. Chem. Soc.* **2005**, *127*, 12492–12493.
26. Dumortier, H.; Lacotte, S.; Pastorin, G.; Marega, R.; Wu, W.; Bonifazi, D.; Briand, J. P.; Prato, M.; Muller, S.; Bianco, A. Functionalized Carbon Nanotubes Are Noncytotoxic and Preserve the Functionality of Primary Immune Cells. *Nano Lett.* **2006**, *6*, 1522–1528.
27. Kam, N. W.; Dai, H. Carbon Nanotubes As Intracellular Protein Transporters: Generality and Biological Functionality. *J. Am. Chem. Soc.* **2005**, *127*, 6021–6026.
28. Kam, N. W. S.; Jessop, T. C.; Wender, P. A.; Dai, H. J. Nanotube Molecular Transporters: Internalization of Carbon Nanotube-Protein Conjugates into Mammalian Cells. *J. Am. Chem. Soc.* **2004**, *126*, 6850–6851.
29. Pantarotto, D.; Singh, R.; McCarthy, D.; Erhardt, M.; Briand, J. P.; Prato, M.; Kostarelos, K.; Bianco, A. Functionalized Carbon Nanotubes for Plasmid DNA Gene Delivery. *Angew. Chem., Int. Ed.* **2004**, *43*, 5242–5246.
30. Kam, N. W.; O'Connell, M.; Wisdom, J. A.; Dai, H. Carbon Nanotubes As Multifunctional Biological Transporters and

near-Infrared Agents for Selective Cancer Cell Destruction. *Proc. Natl. Acad. Sci. U.S.A.* **2005**, *102*, 11600–11605.
31. Kam, N. W. S.; Liu, Z. A.; Dai, H. J. Carbon Nanotubes As Intracellular Transporters for Proteins and DNA: An Investigation of the Uptake Mechanism and Pathway. *Angew. Chem., Int. Ed.* **2006**, *45*, 577–581.
32. Zhao, C.; Peng, Y. H.; Song, Y. J.; Ren, J. S.; Qu, X. G. Self-Assembly of Single-Stranded RNA on Carbon Nanotube: Polyadenylic Acid to Form a Duplex Structure. *Small* **2008**, *4*, 656–661.
33. Wang, X. H.; Ren, J. S.; Qu, X. G. Targeted RNA interference of Cyclin A(2) Mediated by Functionalized Single-Walled Carbon Nanotubes Induces Proliferation Arrest and Apoptosis in Chronic Myelogenous Leukemia K562 Cells. *ChemMedChem* **2008**, *3*, 940–945.
34. Liu, Z.; Winters, M.; Holodniy, M.; Dai, H. siRNA Delivery into Human T Cells and Primary Cells with Carbon-Nanotube Transporters. *Angew. Chem., Int. Ed.* **2007**, *46*, 2023–2027.
35. Pantarotto, D.; Briand, J. P.; Prato, M.; Bianco, A. Translocation of Bioactive Peptides Across Cell Membranes by Carbon Nanotubes. *Chem. Commun.* **2004**, 16–17.
36. Kostarelos, K.; Lacerda, L.; Pastorin, G.; Wu, W.; Wieckowski, S.; Luangsivilay, J.; Godefroy, S.; Pantarotto, D.; Briand, J. P.; Muller, S.; *et al*. Cellular Uptake of Functionalized Carbon Nanotubes Is Independent of Functional Group and Cell Type. *Nat. Nanotechnol.* **2007**, *2*, 108–113.
37. Xiao, H.; Zou, H. F.; Pan, C. S.; Jiang, X. G.; Le, X. C.; Yang, L. Quantitative Determination of Oxidized Carbon Nanotube Probes in Yeast by Capillary Electrophoresis with Laser-Induced Fluorescence Detection. *Anal. Chim. Acta* **2006**, *580*, 194–199.
38. Xiao, H.; Yang, L. S.; Zou, H. F.; Yang, L.; Le, X. C. Analysis of Oxidized Multiwalled Carbon Nanotubes in Single K562 Cells by Capillary Electrophoresis with Laser-Induced Fluorescence. *Anal. Bioanal. Chem.* **2007**, *387*, 119–126.
39. Chaudhary, P. M.; Roninson, I. B. Expression and Activity of P-Glycoprotein, A Multidrug Efflux Pump, In Human Hematopoietic Stem-Cells. *Cell* **1991**, *66*, 85–94.
40. Li, R. B.; Wu, R. A.; Wu, M. H.; Zou, H. F.; Ma, H.; Yang, L.; Le, X. C. MEKC-LIF Analysis of Rhodamine123 Delivered by Carbon Nanotubes in K562 Cells. *Electrophoresis* **2009**, *30*, 1906–1912.
41. Kim, U. J.; Furtado, C. A.; Liu, X.; Chen, G.; Eklund, P. C. Raman and IR Spectroscopy of Chemically Processed Single-Walled Carbon Nanotubes. *J. Am. Chem. Soc.* **2005**, *127*, 15437–15445.
42. Wu, S.; Ju, H. X.; Liu, Y. Conductive Mesocellular Silica-Carbon Nanocomposite Foams for Immobilization, Direct Electrochemistry, And Biosensing of Proteins. *Adv. Funct. Mater.* **2007**, *17*, 585–592.
43. Oh, K. T.; Baik, H. J.; Lee, A. H.; Oh, Y. T.; Youn, Y. S.; Lee, E. S. The Reversal of Drug-Resistance in Tumors Using a Drug-Carrying Nanoparticular System. *Int. J. Mol. Sci.* **2009**, *10*, 3776–3792.
44. Huynh, N. T.; Passirani, C.; Saulnier, P.; Benoit, J. P. Lipid Nanocapsules: A New Platform for Nanomedicine. *Int. J. Pharm.* **2009**, *379*, 201–209.
45. Jabr-Milane, L. S.; van Vlerken, L. E.; Yadav, S.; Amiji, M. M. Multifunctional Nanocarriers to Overcome Tumor Drug Resistance. *Cancer Treat. Rev.* **2008**, *34*, 592–602.
46. Guo, D. D.; Wu, C. H.; Jiang, H.; Li, Q. N.; Wang, X. M.; Chen, B. A. Synergistic Cytotoxic Effect of Different Sized ZnO Nanoparticles and Daunorubicin against Leukemia Cancer Cells under UV Irradiation. *J. Photochem. Photobiol. B* **2008**, *93*, 119–126.
47. Song, M.; Wang, X. M.; Li, J. Y.; Zhang, R. Y.; Chen, B. A.; Fu, D. G. Effect of Surface Chemistry Modification of Functional Gold Nanoparticles on the Drug Accumulation of Cancer Cells. *J. Biomed. Mater. Res., Part A* **2008**, *86A*, 942–946.
48. Chen, B. A.; Cheng, J.; Shen, M. F.; Gao, F.; Xu, W. L.; Shen, H. L.; Ding, J. H.; Gao, C.; Sun, Q.; Sun, X. C.; *et al*. Magnetic Nanoparticle of Fe_3O_4 and 5-Bromotetrandrin Interact Synergistically to Induce Apoptosis by Daunorubicin in Leukemia Cells. *Int. J. Nanomed.* **2009**, *4*, 65–71.
49. Wu, W.; Wieckowski, S.; Pastorin, G.; Benincasa, M.; Klumpp, C.; Briand, J. P.; Gennaro, R.; Prato, M.; Bianco, A. Targeted Delivery of Amphotericin B to Cells by Using Functionalized Carbon Nanotubes. *Angew. Chem., Int. Edit.* **2005**, *44*, 6358–6362.
50. Pastorin, G.; Wu, W.; Wieckowski, S.; Briand, J. P.; Kostarelos, K.; Prato, M.; Bianco, A. Double Functionalization of Carbon Nanotubes for Multimodal Drug Delivery. *Chem. Commun.* **2006**, 1182–1184.
51. Liu, Z.; Chen, K.; Davis, C.; Sherlock, S.; Cao, Q. Z.; Chen, X. Y.; Dai, H. J. Drug Delivery with Carbon Nanotubes for *in Vivo* Cancer Treatment. *Cancer Res.* **2008**, *68*, 6652–6660.
52. Dhar, S.; Liu, Z.; Thomale, J.; Dai, H. J.; Lippard, S. J. Targeted Single-Wall Carbon Nanotube-Mediated Pt(IV) Prodrug Delivery Using Folate as a Homing Device. *J. Am. Chem. Soc.* **2008**, *130*, 11467–11476.
53. Xu, S. Y.; Li, Y. F.; Zou, H. F.; Qiu, J. S.; Guo, Z.; Guo, B. C. Carbon Nanotubes as Assisted Matrix for Laser Desorption/Ionization Time-of-Flight Mass Spectrometry. *Anal. Chem.* **2003**, *75*, 6191–6195.
54. Vermes, I.; Haanen, C.; Steffensnakken, H.; Reutelingsperger, C. A Novel Assay for Apopsis - Flow Cytometric Detection of Phosphatidylserine Expression on Early Apoptotic Cells Using Fluorescein-Labeled Annexin-V. *J. Immunol. Methods* **1995**, *184*, 39–51.
55. Pan, C.; Xu, S.; Hu, L.; Su, X.; Ou, J.; Zou, H.; Guo, Z.; Zhang, Y.; Guo, B. Using Oxidized Carbon Nanotubes As Matrix for Analysis of Small Molecules by MALDI-TOF MS. *J. Am. Soc. Mass Spectrom.* **2005**, *16*, 883–892.
56. Jiang, K. Y.; Schadler, L. S.; Siegel, R. W.; Zhang, X. J.; Zhang, H. F.; Terrones, M. Protein Immobilization on Carbon Nanotubes *via* a Two-Step Process of Diimide-Activated Amidation. *J. Mater. Chem.* **2004**, *14*, 37–39.
57. Ohtani, H.; Ikegawa, T.; Honda, Y.; Kohyama, N.; Morimoto, S.; Shoyama, Y.; Juichi, M.; Naito, M.; Tsuruo, T.; Sawada, Y. Effects of Various Methoxyflavones on Vincristine Uptake and Multidrug Resistance to Vincristine in P-gp-Overexpressing K562/ADM Cells. *Pharm. Res.* **2007**, *24*, 1936–1943.